Likewise, positions parallel to the knife edge imply that $y = 0$, $P_n = z$; and the result is

$$R_{12}^{\parallel} = \exp(-z^2/l^2)$$

It will be noted that in the perpendicular direction, the autocorrelation for the intensities becomes negative at $y = l/(2)^{1/2}$. This result leads to the expectation that a light area would be followed by a dark area within a distance of the order l. Parallel to the knife edge, the intensities remain positively cross-correlated. This combination of results implies that the photograph would tend to exhibit streaking parallel to the knife edge.

The Gaussian model is a convenient mathematical form. A model which is physically justifiable can be developed in the following way.[3] The index of refraction is a function of temperature; the temperature fluctuations may be regarded as a passive conservative additive in the turbulence. Concentration inhomogeneities appear as a result of the action of the velocity field. Thus turbulent velocity spectra, such as the von Kármán formula, describe the index of refraction in the inertial (outer) range. In the inner range the inhomogeneities are dissipated by molecular diffusion. Thus we consider the following model[3] based upon the von Kármán law:

$$C(r) = \begin{cases} 1 - Ar^2, & 0 < r < l_i < l_e \\ [2^{2/3}/\Gamma(1/3)](k_e r)^{1/3} K_{1/3}(k_e r), & l_i < r < \infty \end{cases}$$

where l_i is the inner scale, and for the present purposes its value is of the order of 1 mm. $l_e = 1/k_e$, the outer scale, is about 3 cm, the size of turbulent wakes for small model experiments. The symbol K represents the modified Bessel function with imaginary arguments.

The constant A is found to be

$$A \doteq 0.952\, l_e^{-2/3} l_i^{-4/3}$$

where we have used the fact that for very small $k_e r$ the second part of the correlation function becomes

$$C(r) \approx 1 - [\Gamma(2/3)/\Gamma(4/3)](k_e r/2)^{2/3}$$

The calculation now involves numerical integration of a rather complicated expression for the second derivative of the correlation of the refractive index variations,

$$\partial^2 C(r)/\partial y^2 = \begin{cases} \{-1.904\, l_e^{-2/3} l_i^{-4/3}\}, & 0 \le r \le l_i \\ 0.592\,(k_e r)^{1/3}\{[\frac{1}{3} - 5y^2/9r^2 + \frac{1}{2}(k_e y)^2]K_{1/3}(k_e r)/r^2 + [y^2/3r^2 - 1](k_e/2r) \times [K_{2/3}(k_e r) + K_{4/3}(k_e r)] + (k_e y/2r)^2 [K_{5/3}(k_e r) + K_{7/3}(k_e r)]\}, & l_i \le r < \infty \end{cases}$$

The results of the integration are plotted in Fig. 1 for the case $l_i/l_e = 0.03$. It will be noted that for the von Kármán model the cross correlation in the perpendicular direction again becomes negative, while the parallel correlation remains positive. Thus, the von Kármán model also predicts streaking parallel to the knife edge. In Fig. 2 we plot results for two other cases for different l_i/l_e. Only the perpendicular correlation is shown, since in both cases the parallel correlation remains positive.

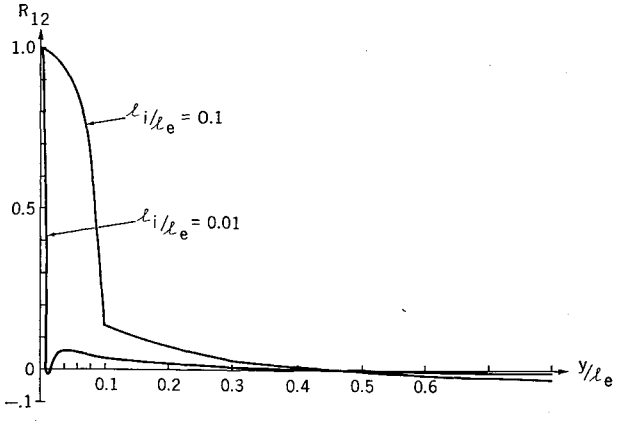

Fig. 2 Autocorrelation for positions perpendicular to the knife edge.

References

[1] Liepmann, H. W. and Roshko, A., *Elements of Gas Dynamics*, Wiley, New York, 1957, pp. 157–160.

[2] Beckmann, P., "Signal Degeneration in Laser Beams Propagated through a Turbulent Atmosphere," *Radio Science Journal of Research*, Vol. 69D, No. 4, April 1965, pp. 629–640.

[3] Tatarski, V. I., *Wave Propagation in a Turbulent Medium*, Pergamon, New York, 1965, Chap. 3.

[4] Gradshteyn, I. S. and Ryshik, I. M., *Table of Integrals, Series and Products*, 4th ed., translated by Scripta Technica Inc., edited by A. Jeffrey, Academic Press, New York, 1965, pp. 1039–1045.

Combustion of an Ablative Fuel in a Constant-Area Channel

Louis J. Spadaccini* and Ely Reiss*
General Applied Science Laboratories Inc., Westbury, N.Y.

Introduction

At present, a considerable amount of interest has been focused on the feasibility of utilizing ablative materials as fuels for hypersonic airbreathing propulsion systems. The ablative serves both as thermal insulation and as a source of fuel for use in force generation schemes. The primary advantage of this concept is the elimination of problems associated with fuel storage, distribution, and injection. A schematic representation of a solid-fueled ramjet engine is shown in Fig. 1. The solid fuel, which comprises the burner portion of the vehicle, is permitted to ablate, mix with the external air, and burn in the main combustion region. The combustion products can then be expanded to provide thrust.

A recent study[1] has demonstrated the feasibility of burning gaseous ablation products in a high-temperature supersonic airstream. Polymethylmethacrylate (PPM) and nylon models were exposed to high-speed wind-tunnel flows. Resulting combustion of the ablation products was found to be efficient and sustainable, and measurements showed significant combustion-induced pressure rises.

The current interest in the combustible ablator concept has generated a need for additional information regarding the fundamental ablation, mixing, and combustion processes. A program was therefore undertaken to further investigate

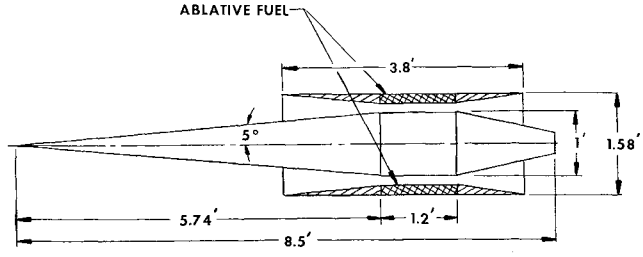

Fig. 1 Schematic of solid-fuel ramjet.

Received May 8, 1969.

* Senior Scientist. Member AIAA.

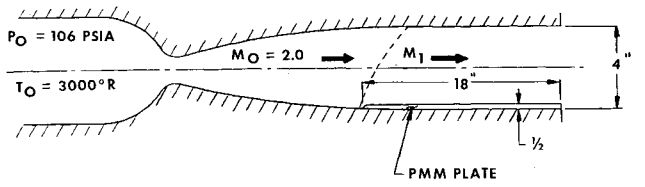

Fig. 2 Schematic of flat-plate test apparatus.

this mode of combustion and gain insight into the magnitude of the pressure increases obtainable.

Experimental Techniques

The experimental program was conducted in a Mach number 2.0, combustion heated, blowdown wind tunnel at nominal stagnation conditions of 106 psia and 1400° to 3300°R. Make-up oxygen was added to provide vitiated air with the correct proportion of atmospheric oxygen. A schematic of the experimental apparatus is shown in Fig. 2. The test section was a 4-in. square, and on one wall a $\frac{1}{2}$-in.-thick PMM plate was mounted. The plate was 18 in. long, 4 in. wide, and had a rounded leading edge. Since the tests were of short duration, and the amount of PMM ablated was small, the phenomenon was considered to be occurring in a constant-area duct. Pressure taps were located on the surface of the model and along the top wall of the test section. The leading edge of the plate produced a curved oblique shock which reflected from the tunnel wall and the plate.

Results

The pressures measured during the test are shown in Fig. 3 and are expressed as pressure coefficients referenced to test section conditions $C_p = (P - P_0)/q_0$ where the subscript 0 denotes freestream conditions. The test labeled "without burning" was run at a stagnation temperature that was high enough to permit ablation but low enough to preclude burning (T_T = 2100°R). An additional test made with cold dry air (T_T = 500°R), so that no ablation occurred, resulted in approximately the same pressures as the test with ablation but no burning. The test labeled "with burning" was run at a stagnation temperature of approximately 3000°R. The occurrence of burning was verified by photographs taken during the test. The difference in measured pressures shown in Fig. 3 (ΔC_p = 0.30 at the end of the plate) is due to combustion of the PPM albation products in the freestream air.

Theoretical calculations of the pressure rise due to combustion of the ablator were made, based on a one-dimensional constant-area heat addition process. The calculations depend on the Mach number M_1 in the constant-area duct at the start of burning. This Mach number is determined by the reduction in area from the test section to the duct and by the recovery η_R of the shocks and reflections produced by the curved leading edge of the plate, that is, the ratio of the total pressures across the shock system. A recovery of 0.80 to 0.85 approximates the pressure loss resulting in M_1 around 1.6. However, since the recovery is not known exactly, M_1

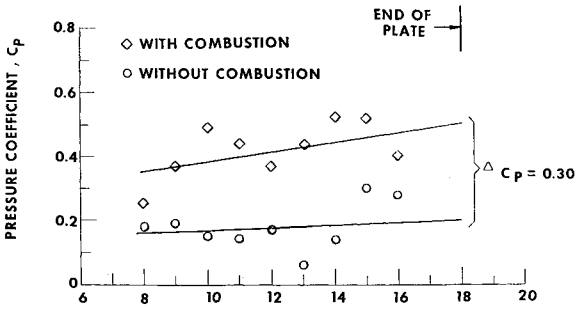

Fig. 3 Experimental values of pressure coefficient on a PMM flat plate.

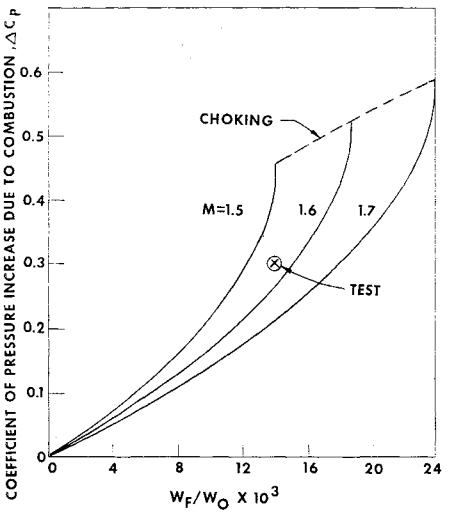

Fig. 4 Combustion ablator fuel/air ratio.

is retained as a parameter in presenting results. The results of the theoretical calculations of the constant-area burning process are shown in Fig. 4 as curves of the pressure rise coefficient ΔC_p vs the ratio of fuel flow to airflow W_f/W_0. The test point indicates the measured value of ΔC_p as deduced from Fig. 3. The test value of W_f/W_0 was determined from the ablation rate W_f and the measured tunnel flow W_0. The ablation rate was determined by weighing the plexiglas plate before and after the test and dividing the difference in weight by the time duration of the test. The results show that the test point is in close agreement with the theoretical results, thereby indicating a relatively efficient combustion process.

In summary, the tests and analysis described herein simulate a rudimentary combustor and provide limited confirmation of the feasibility of utilizing ablative materials as fuels for hypersonic airbreathing propulsion systems.

Reference

[1] Spadaccini, L. and Chinitz, W., "The Combustion of Solid Fuels in a High Temperature Supersonic Air Stream," *AIAA Journal*, Vol. 7, No. 9, Sept. 1969, pp. 1682–1687.

Effective Viscosity in a Turbulent Boundary Layer

S. W. CHI* AND C. C. CHANG†
The Catholic University of America, Washington, D.C.

Nomenclature

C = constant, Eq. (2)
C_f = frictional drag coefficient defined as $2\tau_s/\rho u_G^2$
K = constant, Eq. (1)
l = Prandtl's mixing length, Eq. (7)
P = constant, Eq. (1)
Re_2 = Reynolds number based upon momentum thickness, Eq. (3)
u = velocity in x direction, Eq. (4)
u_G = u in the mainstream
u^+ = nondimensional velocity defined as $u/(\tau_s/\rho)^{1/2}$, Eq. (1)

Received February 3, 1969; revision received June 23, 1969. This work is supported by a National Science Foundation Grant.

* Assistant Professor, Department of Space Science and Applied Physics.
† Professor and Head, Department of Space Science and Applied Physics.